Hindawi
Geofluids
Volume 2023, Article ID 7941695, 10 pages
https://doi.org/10.1155/2023/7941695

Research Article

A Method of Inverting Rock Grain Size Based on Nuclear Magnetic Resonance Logging Data and Application

Jinbo Wu,[1] **Yitao Hu**,[2] **and Hairong Zhang**[3,4]

[1]*Zhanjiang Branch of CNOOC Ltd., Zhanjiang, China*
[2]*Zhanjiang Branch, China France Bohai Geoservices Co., Ltd., Zhanjiang, China*
[3]*Southern Marine Science and Engineering Guangdong Laboratory (Zhanjiang), Zhanjiang, China*
[4]*College of Geophysics and Oil Resources, Yangtze University, Wuhan, Hubei, China*

Correspondence should be addressed to Hairong Zhang; dsq1994@126.com

Received 28 January 2023; Revised 17 May 2023; Accepted 18 May 2023; Published 12 June 2023

Academic Editor: Tianshou Ma

Rock grain size parameter is the key parameter of reservoir rock physics analysis. The study found that the relationship between the NMRT_2spectrum and rock grain size distribution curve is directly related to NMRT_2distribution and grain size distribution of rock, so you can use T_2 to retrieve the size distribution of rock NMR spectral data. Based on the calculation of the rock core experiment results of grain size distribution by NMR T_2 distribution using the conversion method of piecewise nonlinear calibration for each core, adjusting the calibration parameters to make the grain size distribution calculated with the core analysis of grain size distribution approximation, the error is minimum to obtain each core scale parameter conversion. In the end, the core parameters are classified according to the parameters of pore and permeability. Finally, according to the actual NMR T_2 distribution curve inversion of underground rock granularity, the inversion results contrast with the core analysis results, and the reliability of the method is verified to provide accurate, continuous rock size distribution profile analysis of geological reservoir rock physics.

1. Introduction

Grain size data are widely used in the research of stratigraphic petrophysics and play an important role in the theory of sediment classification and nomenclature, identification of paleogeographic environment, analysis of sedimentation, evaluation of reservoir quality, etc. [1, 2]. In addition, the grain size of rock has a great influence on diagenesis and plays an important role in restricting the physical properties of rock and the changing characteristics of its pore structure. It can be seen that the rock grain size parameter is the key evaluation parameter of reservoir petrophysical analysis. Since high-temperature and high-pressure formations [3–6] are widely developed in the Yinggehai-Qiongdongnan Basin and the mud proportion used in the drilling process is up to 2.0, this high-temperature and high-pressure mud system has a high content of barite and heavy ore components, which causes obvious problems in determining the grain size of logging rock, and the error of logging profile obtained is large, bringing a series of problems to the subsequent petrophysical analysis. At present, the techniques for obtaining rock grain size mainly include experimental analysis and logging data. The experimental analysis techniques mainly include laser grain size analysis and sieve analysis. Zhao et al. [7], Chen et al. [8], and Luo et al. [9] used logging curves such as natural gamma ray and flushing resistivity to model with median grain size, and Ning et al. [10] proposed to use natural gamma ray curves to obtain grain size parameters through wavelet transform. However, the above methods obtain few grain size parameters, which cannot truly reflect the vertical combination characteristics of the formation. Given the existing characteristics and problems of the reservoir in the Yinggehai-Qiongdongnan Basin in the western sea area of the South China Sea, this paper studies the relationship between the nuclear magnetic resonance T_2 spectrum of the core and the rock grain size distribution curve and calculates the rock grain size distribution from the nuclear magnetic T_2 distribution for each core by using the

subsection nonlinear scale conversion method, obtains the conversion scale parameters of each core, classifies the core in combination with the porosity and permeability parameters, and determines the scale parameters of each type of core. A model for continuous calculation of rock grain size distribution from nuclear magnetic logging data is established. The reliability of this method is proved by the test and application of actual data.

2. Methodology

According to the NMR relaxation mechanism, the lateral relaxation time T_2 obtained from nuclear magnetic logging [11] is as follows:

$$\frac{1}{T_2} = \frac{1}{T_{2B}} + \rho_2\left(\frac{S}{V}\right) + \frac{D(\gamma G T_E)^2}{12}, \quad (1)$$

where T_{2B} is the volume (free) relaxation time of fluid, D is the diffusion coefficient, G is the magnetic field gradient, T_E is the echo interval, S is pore surface area, V is the pore volume, ρ_2 is the transverse surface relaxation strength of rock, and T_2 is the transverse relaxation time.

The value of T_{2B} in the actual stratum is usually in the range of 2000-3000 ms, which is much larger than T_2, i.e., $T_{2B} >> T_2$. Therefore, the first term on the right side in Equation (1) can be neglected. If there is a significant diffusion effect on the relaxation of water in spin echo measurement, due to the diffusion effect, the T_2 distribution shifts towards the short T_2 direction, and in order to correctly evaluate the aperture distribution, it is necessary to use a short echo time for measurement. The current nuclear magnetic logging tool has a minimum echo time of only 0.1 to 0.2 ms, at which time the diffusion effect can be completely ignored. The nuclear magnetic resonance data in the study area described in the paper are all obtained using the CMR-PLUS instrument of Schlumberger Company. The magnetic field of the logging tool is uniform, and the formation wettability in the study area is of hydrophilic type. Therefore, the G value corresponding to Equation (1) is very small, and T_E is short enough [12]. Therefore, the third term in Equation (1) can also be ignored. For the simple mineralogy of 100% quartz sand, the transverse relaxation time is directly related to the specific surface S/V of the pores, which can be expressed as follows:

$$\frac{1}{T_2} = \rho_2\left(\frac{S}{V}\right). \quad (2)$$

From Equation (2), it can be seen that the relaxation time T_2 is related to the size and shape of the pore space [13–24]. It is assumed that the rock in the formation consists of an ideal accumulation of spherical grains, as shown in Figures 1 and 2.

The ratio of the specific surface of rock grains to the total volume of rock grains can be derived from the volume model (see Equation (3)). And the parameters of rock pore surface area and pore volume can be obtained by converting

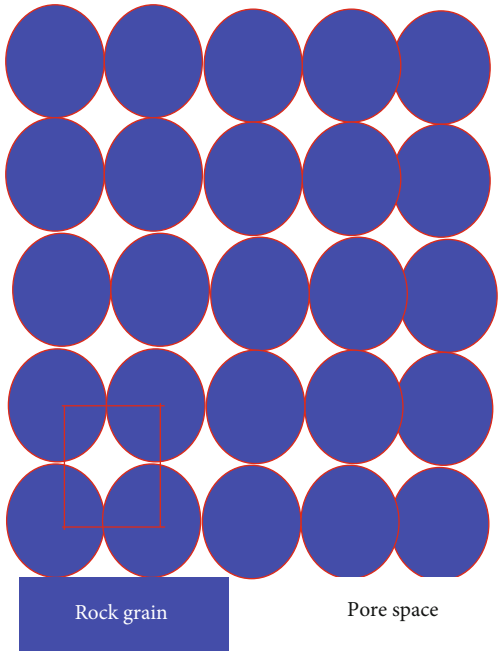

Figure 1: Schematic diagram of rock grain cube accumulation.

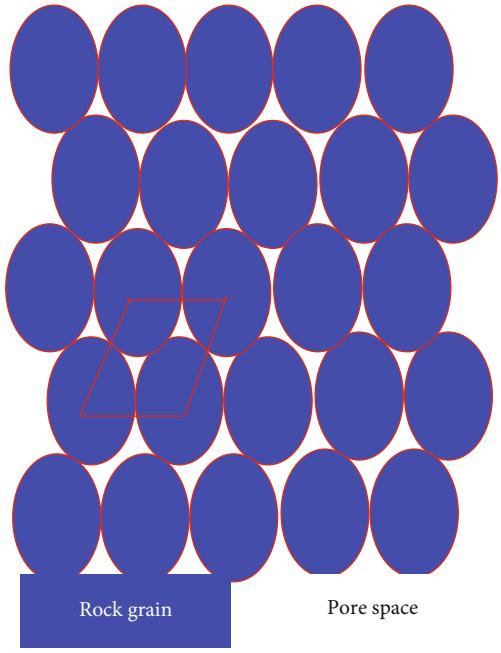

Figure 2: Schematic diagram of italic accumulation of rock grains.

the specific surface of rock grains, the total volume of grains, and rock porosity, as shown in Equation (4). Therefore, the relationship between rock pore surface area, pore volume, and rock grain size can be obtained from Equation (3), Equation (4), and Equation (5). Combining Equation (2), the calculation model of the nuclear magnetic transverse relaxation time T_2 and the rock grain size can be obtained, which is shown in Equation (6). Rock grains are influenced by sediment sources as well as late diagenesis, resulting in the regular accumulation of rock grains in the stratum that are not exactly round. Therefore, to correct for these effects,

Table 1: Basic data of experimental cores.

No.	Porosity (%)	Permeability (mD)	Lith	No.	Porosity (%)	Permeability (mD)	Lith	No.	Porosity (%)	Permeability (mD)	Lith
1	18.1	37.00	Silty fine sandstone	15	18.7	1.76	Siltstone	29	19.6	16.60	Silty fine sandstone
2	15.8	0.11	Argillaceous siltstone	16	19.9	2.32	Silty fine sandstone	30	20.4	2.07	Siltstone
3	18.1	1.38	Silty fine sandstone	17	20.3	6.39	Silty fine sandstone	31	19.5	2.52	Siltstone
4	11.4	0.03	Argillaceous siltstone	18	19.3	2.32	Fine sandstone	32	20.5	6.14	Fine sandstone
5	17.4	2.72	Siltstone	19	20.4	4.79	Fine sandstone	33	20.7	8.18	Fine sandstone
6	21.2	121.00	Silty fine sandstone	20	17.0	0.13	Siltstone	34	20.1	2.86	Fine sandstone
7	21.8	186.00	Silty fine sandstone	21	16.3	0.16	Siltstone	35	20.1	2.49	Fine sandstone
8	19.3	93.60	Siltstone	22	11.5	0.10	Argillaceous siltstone	36	19.5	29.90	Fine sandstone
9	20.5	122.00	Silty fine sandstone	23	17.3	0.20	Siltstone	37	20.2	11.60	Silty fine sandstone
10	19.9	110.00	Silty fine sandstone	24	14.7	0.12	Argillaceous siltstone	38	20.1	15.50	Silty fine sandstone
11	17.5	11.70	Siltstone	25	19.5	15.20	Silty fine sandstone	39	19.9	10.00	Silty fine sandstone
12	20.2	2.03	Fine sandstone	26	19.7	16.70	Fine sandstone	40	19.7	3.83	Siltstone
13	18.8	1.62	Silty fine sandstone	27	20.1	19.90	Silty fine sandstone	41	19.7	3.96	Siltstone
14	14.5	0.13	Argillaceous siltstone	28	19.3	12.90	Silty fine sandstone				

Table 2: Mineralogy of the experimental cores.

No.		1	2	3	4	5	6	7	8	9	10	11	12	13	14
Mineralogy (%)	Quartz	87.0	75.0	74.0	65.0	80.0	90.0	90.0	88.0	91.0	88.0	83.0	75.0	77.0	70.0
	Feldspar	4.0	6.0	5.0	9.0	5.0	2.0	3.0	3.0	3.0	4.0	3.0	6.0	5.0	6.0
	Carbonate	5.0	4.0	7.0	7.0	5.0	3.0	3.0	4.0	3.0	5.0	4.0	4.0	5.0	6.0
	Clay	4.0	15.0	14.0	19.0	10.0	5.0	4.0	5.0	3.0	3.0	10.0	15.0	13.0	18.0
No.		15	16	17	18	19	20	21	22	23	24	25	26	27	28
Mineralogy (%)	Quartz	77.0	79.0	81.0	81.0	85.0	65.0	65.0	65.0	64.0	65.0	88.0	86.0	86.0	84.0
	Feldspar	5.0	7.0	6.0	5.0	4.0	10.0	12.0	10.0	11.0	10.0	2.0	3.0	4.0	4.0
	Carbonate	5.0	3.0	4.0	6.0	4.0	6.0	6.0	6.0	6.0	6.0	4.0	4.0	4.0	4.0
	Clay	13.0	11.0	9.0	9.0	7.0	19.0	17.0	19.0	19.0	19.0	6.0	7.0	6.0	8.0
No.		29	30	31	32	33	34	35	36	37	38	39	40	41	
Mineralogy (%)	Quartz	84.0	80.0	76.0	82.0	82.0	76.0	78.0	87.0	84.0	84.0	80.0	78.0	80.0	
	Feldspar	4.0	6.0	7.0	5.0	5.0	8.0	7.0	4.0	5.0	5.0	7.0	6.0	7.0	
	Carbonate	4.0	4.0	4.0	4.0	4.0	4.0	4.0	4.0	3.0	3.0	3.0	4.0	3.0	
	Clay	8.0	10.0	13.0	9.0	9.0	12.0	11.0	5.0	8.0	8.0	10.0	12.0	10.0	

an influence factor CF parameter is added to Equation (6), which leads to Equation (7). It is clear that the rock grain size is related to the NMR T_2 time, ρ_2 rock transverse surface relaxation strength, rock porosity ϕ, and the correction factor CF. When calculating the rock grain size distribution using Equation (7) for the NMR T_2 data, it is also necessary

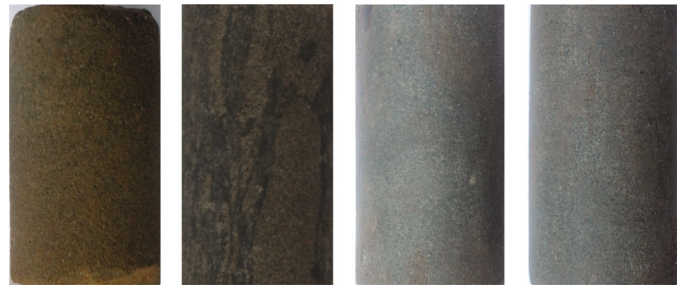

Figure 3: Core photos for experimental analysis.

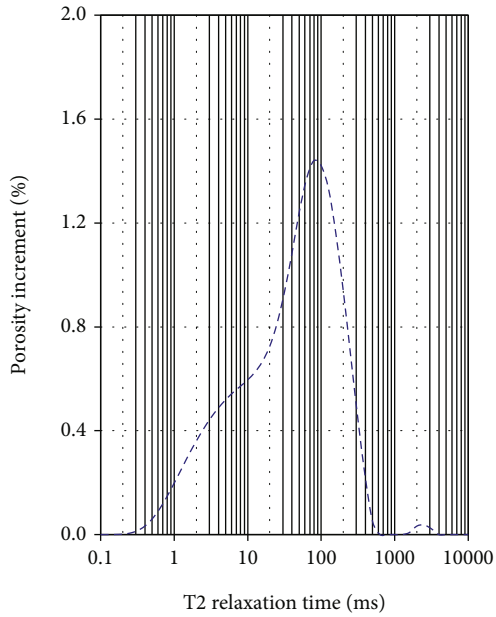

Figure 4: Nuclear magnetic resonance T_2 spectrum.

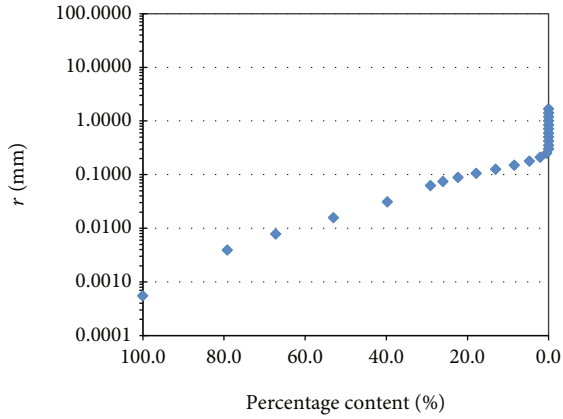

Figure 5: Grain size distribution.

to obtain accurate ρ_2 and CF parameters. Chen et al. [25] pointed out that the ρ_2 parameter is affected by the rock mineral fraction, resulting in a wide range of distribution of this value, which is not easy to determine. Therefore, the conversion factor C value in Equation (8) needs to be determined by interscaling the NMR and grain size experiments. Forty-one representative cores in the region were selected for simultaneous NMR and grain size analysis experiments to obtain the aforementioned C values.

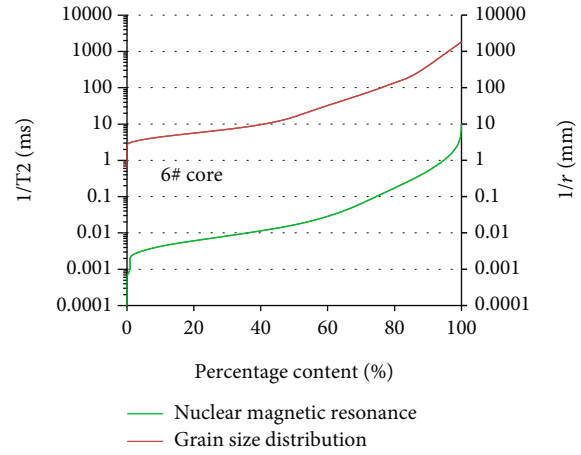

Figure 6: Comparison diagram of nuclear magnetic resonance T_2 and particle size distribution of core 6#.

$$\frac{S_{\text{matrix}}}{V_{\text{matrix}}} = \frac{4\pi r_{\text{grain}}^2}{4/3\pi r_{\text{grain}}^3} = \frac{3}{r_{\text{grain}}}, \tag{3}$$

$$\frac{S}{V} = \frac{S_{\text{matrix}}}{V_{\text{matrix}}} * \frac{1-\varnothing}{\varnothing}, \tag{4}$$

$$\frac{S}{V} = \frac{3}{r_{\text{grain}}} * \frac{1-\varnothing}{\varnothing}, \tag{5}$$

$$\frac{1}{\rho_2 T_2} = \frac{3}{r_{\text{grain}}} * \frac{1-\varnothing}{\varnothing}, \tag{6}$$

$$\frac{1}{\rho_2 T_2} = \text{CF} * \frac{3}{r_{\text{grain}}} * \frac{1-\varnothing}{\varnothing}, \tag{7}$$

$$r_{\text{grain}} = C * T_2 * \frac{1-\varnothing}{\varnothing}, \tag{8}$$

where S_{matrix} is the surface area of rock grains, V_{matrix} is the volume of rock grains, r_{grain} is the grain size of rock grains, π is the circumference, S is the pore surface area, V is the pore volume, ϕ is the porosity of rock, ρ_2 is the transverse surface

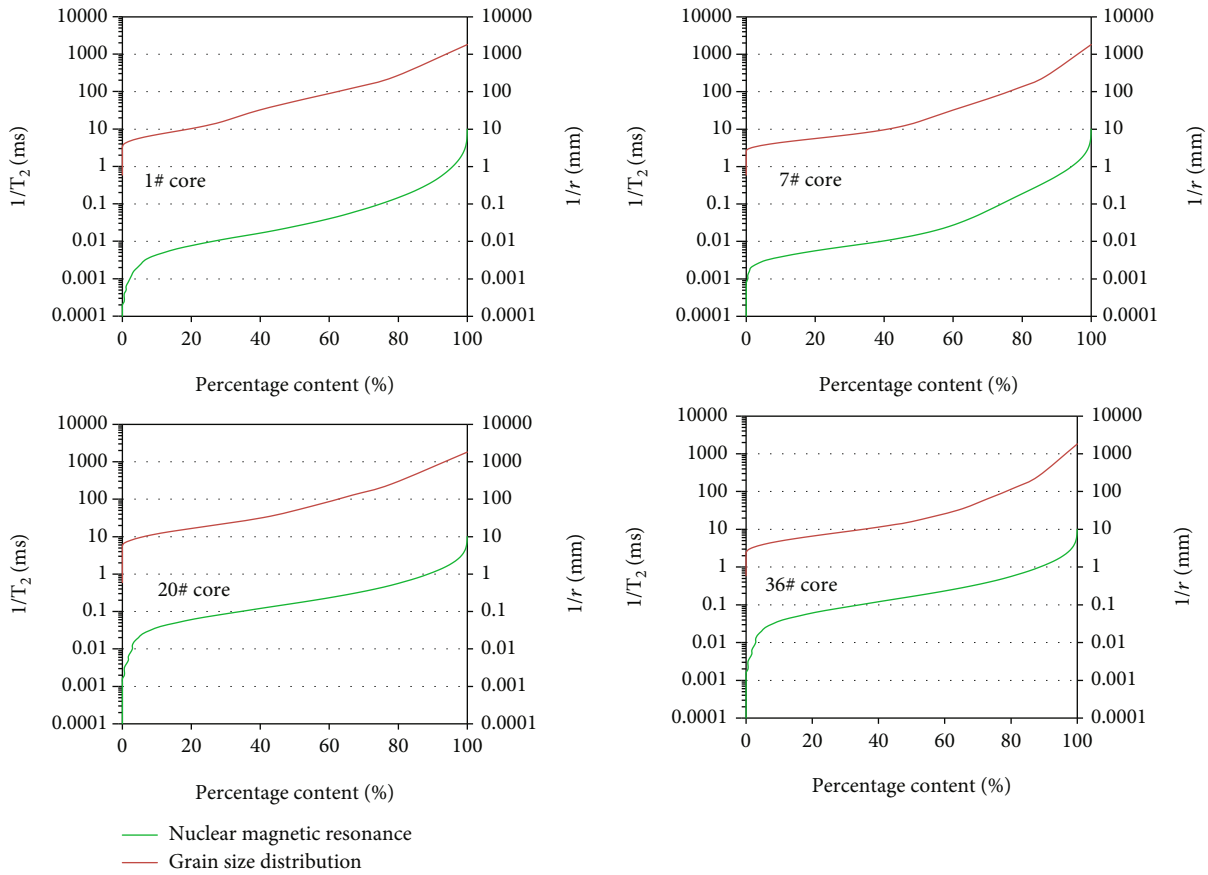

Figure 7: Comparison of NMR T_2 spectrum and grain size distribution.

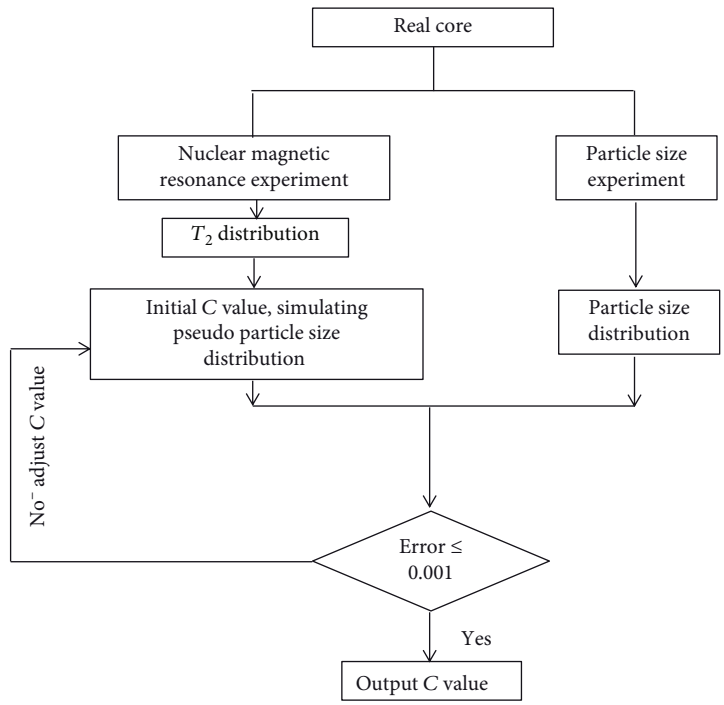

Figure 8: Flow chart of the method to determine the C value.

Table 3: Statistical table of conversion coefficient C of the experimental core analysis.

No.	Depth (m)	Porosity (%)	Permeability (mD)	The value of C		No.	Depth (m)	Porosity (%)	Permeability (mD)	The value of C	
				$T_2 \le 50$ ms	$T_2 > 50$ ms					$T_2 \le 50$ ms	$T_2 > 50$ ms
1	3218.0	18.1	37	0.0003	0.00025	22	2906.54	11.5	0.1	0.0006	0.0005
2	3359.0	15.8	0.11	0.0006	0.0005	23	2908.96	17.3	0.2	0.0006	0.0005
3	3433.0	18.1	1.38	0.00025	0.0004	24	2911.21	14.7	0.12	0.0006	0.0005
4	3068.6	11.4	0.03	0.0006	0.0005	25	2863.88	19.5	15.2	0.00025	0.0004
5	3126.48	17.4	2.72	0.00025	0.0004	26	2865.93	19.7	16.7	0.00025	0.0004
6	3077.45	21.2	121	0.0003	0.00025	27	2867.72	20.1	19.9	0.00025	0.0004
7	3079.47	21.8	186	0.0003	0.00025	28	2868.9	19.3	12.9	0.00025	0.0004
8	3081.15	19.3	93.6	0.0003	0.00025	29	2871.08	19.6	16.6	0.00025	0.0004
9	3084.15	20.5	122	0.0003	0.00025	30	2862.14	20.4	2.07	0.00025	0.0004
10	3087.54	19.9	110	0.0003	0.00025	31	2865.01	19.5	2.52	0.00025	0.0004
11	3091.55	17.5	11.7	0.0003	0.0004	32	2866.57	20.5	6.14	0.00025	0.0004
12	2980.52	20.2	2.03	0.0003	0.0004	33	2869.1	20.7	8.18	0.00025	0.0004
13	2991.11	18.8	1.62	0.0003	0.0004	34	2871.06	20.1	2.86	0.00025	0.0004
14	2992.57	14.5	0.13	0.0006	0.0005	35	2876.07	20.1	2.49	0.00025	0.0004
15	3034.65	18.7	1.76	0.0003	0.00025	36	2907.3	19.5	29.9	0.0003	0.0004
16	3039.14	19.9	2.32	0.0003	0.00025	37	2911.08	20.2	11.6	0.0003	0.0004
17	3041.72	20.3	6.39	0.0003	0.00025	38	2914.75	20.07	15.5	0.0003	0.0004
18	3045.7	19.3	2.32	0.0003	0.00025	39	2918.24	19.94	10	0.0003	0.0004
19	3049	20.4	4.79	0.0003	0.00025	40	2921.26	19.73	3.83	0.0006	0.0005
20	2900.72	17	0.13	0.0006	0.0005	41	2923.61	19.72	3.96	0.0003	0.0004
21	2903.55	16.3	0.16	0.0006	0.0005						

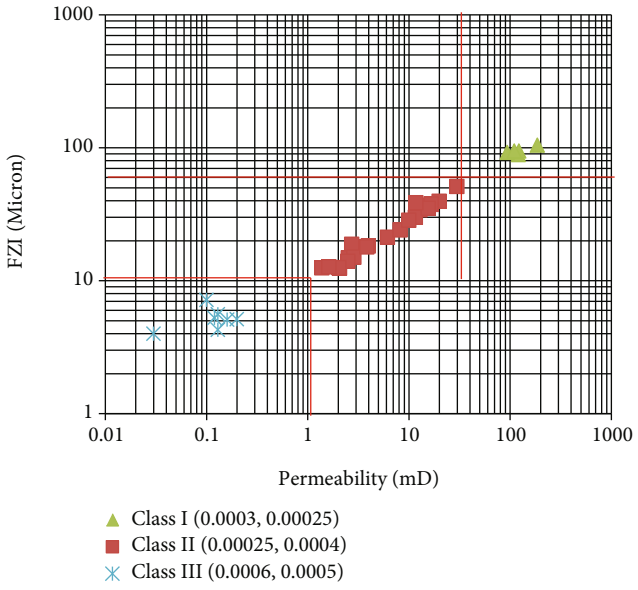

Figure 9: Diagram of the relationship between the conversion coefficient C and the core physical properties.

relaxation strength of rock, T_2 is the transverse relaxation time, CF is the correction factor, and C is the conversion factor, $C = \mathrm{CF} \times \rho_2 \times 3$. From Equation (8), the rock size distribution can be approximated under the condition that the T_2 distribution is known.

Table 4: C value of different types of reservoirs.

Type	C value of conversion coefficient	
	$T_2 \le 50$ ms	$T_2 > 50$ ms
I	0.0003	0.00025
II	0.00025	0.0004
III	0.0006	0.0005

3. NMR and Grain Size Analysis Experiments

3.1. Sampling Background. The buried depth of the Huangliuzu Formation reservoir in the Yinggehai-Qiongdongnan Basin in the west of the South China Sea is 2700-3200 m, and the compaction diagenesis is strong, resulting in the complex pore structure of the Huangliuzu Formation reservoir. In the early stage, operators obtained abundant physical core data from the Huangliuzu Formation reservoir by drilling or sidewall coring and selected a certain amount of cores to carry out nuclear magnetic resonance, particle size analysis, and other experiments, forming the core analysis database of Liushagang Formation. In this study, 41 core samples that can represent the characteristics of regional reservoir and measure nuclear magnetic resonance and grain size were selected from the database as the research data. The core lithology is argillaceous siltstone, silty fine sandstone, siltstone, fine sandstone, etc. The porosity distribution range is 11.5%~20.7%, as shown in Table 1. The XRD

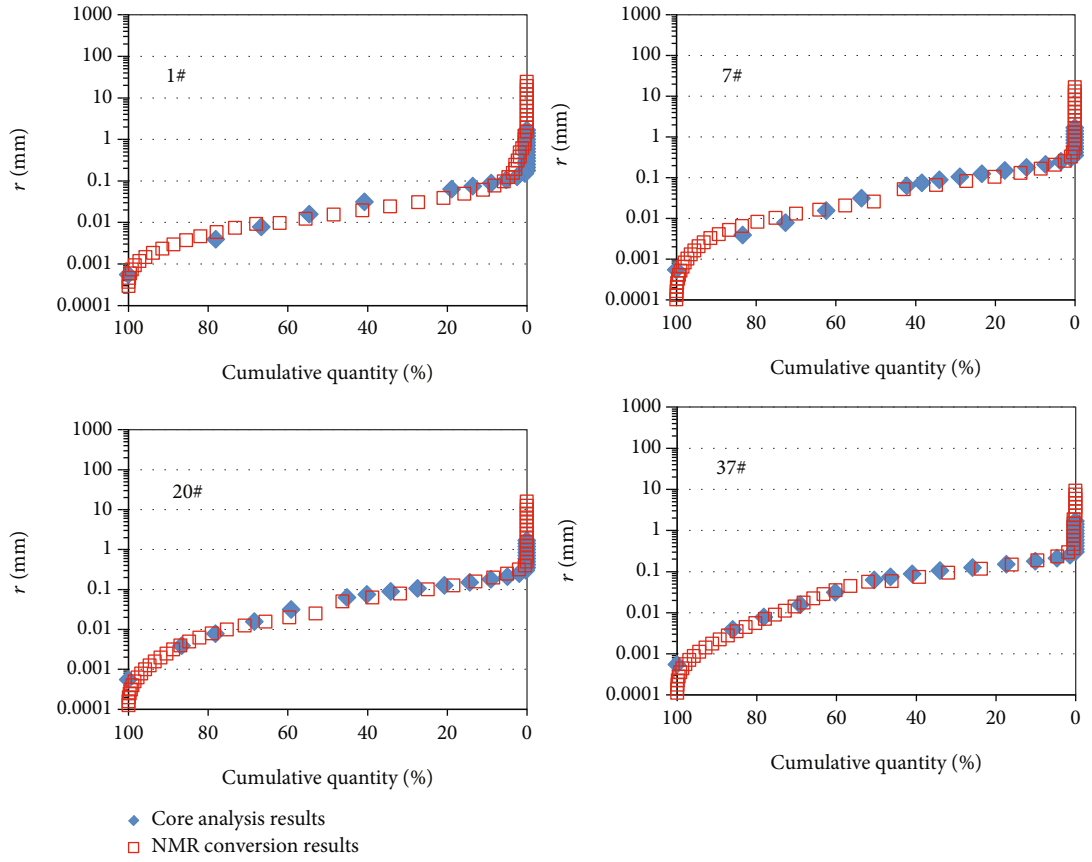

Figure 10: Comparison of grain size distribution between T_2 NMR distribution and core grain size distribution.

mineralogy of the core samples in this study is listed in Table 2. From the table, it can be seen that the mineral composition of the core is mainly composed of quartz, there is a certain amount of feldspar and clay minerals in the low permeability rock core. Figure 3 shows four representative core photos. The core nuclear magnetic experiment described in this paper is measured by the CoreSpec-1000 NMR core analyzer of NUMAR Company in the United States. The echo interval selected in the experiment is 0.1 ms. The waiting time, receiving grain, and echo string length are selected according to different cores. The gain size experiment was measured by laser method.

3.2. Interrelationship between T_2 Distribution and Grain Size Distribution. From Equation (8), it can be seen that under the condition that the nuclear magnetic resonance T_2 spectrum is known, the rock grain size distribution curve can be approximately obtained, which is called the rock grain size distribution curve. The nuclear magnetic resonance T_2 spectrum has a close correlation with the rock grain size distribution curve. To illustrate the rationality of Equation (8), the nuclear magnetic resonance T_2 spectrum and grain size distribution curve of core are analyzed. Figures 4 and 5 show the nuclear magnetic resonance T_2 spectrum of core 6# and obtain the grain size distribution curve of rock through grain size experiments. In order to more intuitively see the relationship between core nuclear magnetic resonance T_2 spectrum and grain size distribution curve, it is necessary to preprocess these two experimental data. Firstly, convert the porosity increment parameter in the ordinate of Figure 4 into a porosity percentage distribution parameter, and convert T_2 to $1/T_2$. Then, convert the rock grain size r in Figure 5 to $1/r$. Finally, the nuclear magnetic resonance T_2 spectrum and grain size distribution curve after conversion coordinate calibration are made into a cross plot, as shown in Figure 6. In Figure 6, there are two ordinates, with $1/T_2$ value on the left, and the unit is ms. On the right is the reciprocal $1/r$ value of grain size, in mm. The abscissa is the percentage content. Similarly, the nuclear magnetic resonance T_2 and rock grain size distribution curves of 41 cores described in Table 1 are processed. Figure 7 shows the overlapping comparison diagram of T_2 distribution and grain size distribution of 4 rock samples (nos. 1, 7, 20, and 36 in Table 1). From the figure, it can be seen that the change patterns of the two are very similar or similar, indicating that there is a close correlation between the two, so it is feasible to convert the rock grain size distribution curve through nuclear magnetic resonance T_2.

4. Methods for Determining the Conversion Factor C

The grain size distribution and NMR T_2 distribution data obtained experimentally from 41 cores were analyzed, and

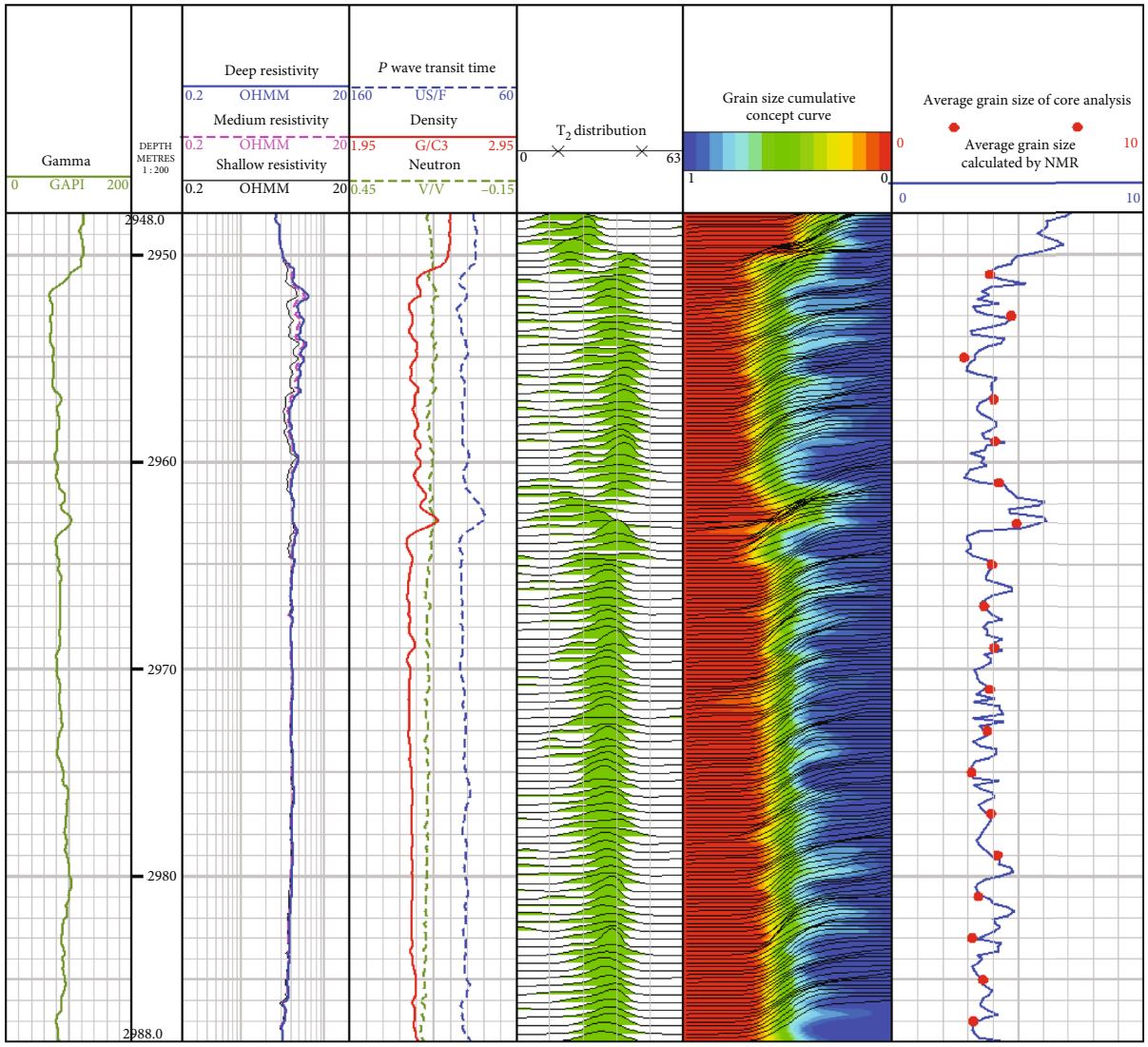

Figure 11: Calculation results of rock grain size distribution in well XF-11.

the flow of the method to determine the conversion factor C value is shown in Figure 8. The main steps are as follows: (i) determine the interval of the conversion factor C value, (ii) change the C value according to the specified step to obtain the pseudo size distribution curve, and (iii) calculate the error between the NMR simulation pseudo size distribution curve and the experimental size distribution. If the error is less than the given cutoff value, the C value is output; otherwise, it returns to (ii) until the calculated error is less than the cutoff value. At this point, the rock size distribution curve is obtained by substituting the C value into Equation (8).

During the actual data processing of the cores, the NMR T_2 distribution needs to be processed in two stages. The T_2 cutoff point is 50 ms, i.e., the conversion factor C values for $T_2 \le 50$ ms and $T_2 > 50$ ms are not the same. The cores were processed and analyzed using the above method flow to obtain the conversion factor C values for each core, as shown in Table 3.

The flow zone index (FZI) is one of the effective parameters to describe the reservoir pore structure and is defined as follows:

$$\mathrm{FZI} = \frac{1-\varnothing}{\varnothing}\sqrt{\frac{K}{\varnothing}}, \tag{9}$$

where ϕ is the rock porosity, K is the permeability, and FZI is the flow zone index. Combined with the core porosity and permeability parameters, the conversion coefficient C values of 41 cores were analyzed in depth. The cores were classified into three types, as shown in Figure 9: class I: 60 < FZI, 30 mD < K; class II: 10 ≤ FZI ≤ 60, 1 mD ≤ K ≤ 30 mD; and class III: FZI ≤ 10, K < 1 mD.

It was found that the conversion factor C values were fixed for each type of core, as shown in Table 4.

The 41 cores in Table 1 were processed using Equation (8) and the conversion factors in Table 3. Figure 10 shows

the NMR T_2 distribution converted grain size of four of the cores compared with the grain size distribution of the core experiment. The red square dots are the grain size distribution curves obtained from the NMR T_2 distribution calculations, and the blue solid dots are the grain size distribution curves obtained from the core experimental analysis. Analysis of Figure 10 shows that the grain size distribution curves calculated by NMR T_2 distribution and the core experimental grain size distribution curves are in good agreement in terms of morphology and change trend.

5. An Application into Well Profile

To test the accuracy of the method in this paper, the rock grain size results calculated by this method are compared with the grain size test data. Figure 11 shows the results of the interpretation using the NMR logging data of well XF-11 processed according to the method in this paper; through geological logging, it can be seen that the lithology of the calculated processing layer is fine sandstone, with quartz as the main rock mineral and clay content less than 5%. The fifth panel shows the logging lithology, the sixth panel shows the NMR logging T_2 spectrum, and the seventh panel shows the calculated grain size accumulation probability curve. The solid red dots in the eighth lane are the mean grain size (Φ) of the core analysis, and the solid blue line is the mean grain size (Φ) curve calculated based on the NMR logging data. It can be seen that the logging calculation results are consistent with the core experimental analysis grain size averages. The absolute error between the mean grain size (Φ) of 19 cores and the mean grain size (Φ) calculated from the logs is 0.12. Based on the logs, natural gamma, and triple porosity curves, the lithology of well section 2961.5-2963.2 m is mudstone. The average value of the grain size (Φ) calculated from the logs is different from the reservoir section. There is a core at the depth of 2963 m, and the core analysis results are also in good agreement with the calculation results. It is known that the method of continuous calculation of downhole rock size distribution by NMR T_2 distribution is reliable and can provide accurate continuous rock grain size distribution profiles for petrophysical analysis of geological reservoirs.

6. Conclusions

(1) The grain size distribution in the actual formation is affected by many factors leading to its complex variation characteristics. For the quartz dominated core samples, core experiments indicate that there is a good correlation between the NMR T_2 distribution and the rock size distribution curve

(2) Combined with the core experimental data, the conversion coefficients of NMR T_2 distribution to grain size distribution for three types of reservoirs were obtained by using the segmented nonlinear fitting method. The comparison of the NMR conversion results with the core experimental results has good similarity, which verifies the reliability of the method

(3) Applying the method to well logging data, the grain size distribution curve of downhole rocks can be calculated continuously, and then, the grain size parameters of the formation can be evaluated quantitatively. The results are in good agreement with the results of the assay analysis. In the reservoirs dominated by quartz, comparative analysis shows that the method can obtain reliable grain size distribution curves from T_2 distribution with high accuracy. For complex lithologic reservoirs, it is necessary to analyze the applicability of the method based on actual core results to obtain reliable calculation results

Data Availability

The original contributions presented in the study are included in the article/supplementary material. Further inquiries can be directed to the corresponding author.

Conflicts of Interest

The authors declare that there is no conflict of interest regarding the publication of this paper.

Acknowledgments

This study was funded by the "Research and development of key technologies and equipment of marine vibroseis system," a key project of Guangdong Provincial High Quality Economic Development Promotion Project (Marine Economic Development) in 2022 (Grant No. GDNRC2022029).

References

[1] Z. Q. Song, J. L. Yang, L. L. Pan, X. W. Lu, and J. Wang, "Study on the favorable sedimentary facies belt of conglomerate reservoir by using grain-size analysis data," *Oil & Gas Recovery Technology*, vol. 12, no. 6, pp. 16–19, 2005.

[2] X. Wang, G. M. Fu, and A. H. Guo, "Research on determination of effective thickness for oil reservoirs with low permeability: a case of Chang-2 reservoir of Ansai oilfield," *Reservoir Evaluation and Development*, vol. 8, no. 6, pp. 1–6, 2018.

[3] Y. H. Xie, "Models of pressure prediction and new understanddings of hydrocarbon accumulation in the Yinggehai basin with hingh temperature and super-high pressure," *Natural Gas Industry*, vol. 31, no. 12, pp. 21–25, 2011.

[4] F. C. Luo, X. Chen, Z. Shi et al., "Effects of precipitation and dissolution of carbonate cements on the quality of deeply buried high-temperature and overpressured clastic reservoirs: XD 10 block, Yinggehai basin, South China Sea," *Marine and Petroleum Geology*, vol. 139, article 105591, 2022.

[5] X. Zhao, G. Yao, X. Chen, R. Zhang, Z. Lan, and G. Wang, "Diagenetic facies classification and characterization of a high-temperature and high-pressure tight gas sandstone reservoir: a case study in the Ledong area, Yinggehai basin," *Marine and Petroleum Geology*, vol. 140, article 105665, 2022.

[6] F. Li, F. Zhou, Y. S. Li, W. Guo, and S. Z. Huang, "Sonic velocity prediction while drilling at high temperature and overpressure formation," *Offshore oil*, vol. 39, no. 1, pp. 61–65, 2019.

[7] J. Zhao, C. W. Xiao, M. Wang, and W.-Z. Chen, "Application of logging data to the sediment size-grading inversion," *Earth Science (Journal of China University of Geosciences)*, vol. 38, no. 4, pp. 792–796, 2013.

[8] G. Y. Chen, Y. L. Zhou, and Y. Hu, "The petrophysics characterization of clastic reservoir and the methods of lithology," *Journal of Southwest Petroleum University (Science & Technology Edition)*, vol. 33, no. 2, pp. 21–27, 2011.

[9] L. Luo, X. W. Zhu, J. Chang, Z. Y. Zhou, and Z. P. Hu, "Logging recognition methods for clastic rocks with different granularities in blocks su-5 and tao-7," *Natural Gas Industry*, vol. 27, no. 12, pp. 36–38, 2007.

[10] Y. A. Ning, W. A. Gui-Wen, L. A. Jin, L. I. Jian-Lun, C. A. Dan, and J. I. Ji-Jun, "Application of gamma curves wavelet transform to calculate grain size parameters," *Geoscience*, vol. 26, no. 4, pp. 778–783, 2012.

[11] L. Z. Xiao, *NMR Imaging Logging Principles and Applications*, Science Press, Beijing, 1998.

[12] C. R. Coates and D. L. Miller, *Applying log measurements of restricted diffusion and T_2 to formation evaluation. SPWLA 36th Annual Logging Symposium*, 1995.

[13] B. Purkait, "Grain-size distribution patterns of a point bar system in the Usri River, India," *Earth Surface Processes and Landforms*, vol. 31, no. 6, pp. 682–702, 2006.

[14] T. Conroy, Y. Mahabeer, K. Seth, and P. Miklavs, "Using nuclear magnetic resonance data for grain size estimation and expandable sand screen design," *SPWLA 51st Annual Logging Symposium*, 2010.

[15] M. Gladkikh, *A Priori Prediction of Macroscopic Properties of Sedimentary Rockscontaining Two Immiscible Fluid*, University of Texasat Austin, Austin, TX, USA, 2005.

[16] L. Wu, W. Krijgsman, J. Liu, C. Li, R. Wang, and W. Xiao, "CFLab: a MATLAB GUI program for decomposing sediment grain size distribution using Weibull functions," *Sedimentary Geology*, vol. 398, article 105590, 2020.

[17] M. Babs Oyeneyin, C. Macleod, G. Oluyemi, and A. Onukwu, "Intelligent sand management," in *29thAnmual SPE International Techmical Conference and Exhibition*, Abuja, Nigeria, 2005.

[18] W. Thungsuntonkhun and T. W. Engler, "Applying NMR-hydraulic flow unit technique to estimate J-function and capillary pressure," in *SPWLA 45th Annual Logging Symposium*, Noordwijk, Netherlands, 2004.

[19] W. Klopf, "CMR tool brings new insightinto reservoir properties," in *Italy Reservoir Optimization Conference*, Venice ,Italy, 2000.

[20] G. Li, R. Du, J. Tang et al., "Comparison of the graphic and moment methods for analyzing grain-size distributions: a case study for the Chinese inner continental shelf seas," *International Journal of Sediment Research*, vol. 37, no. 6, pp. 729–736, 2022.

[21] J. Pszonka, B. Schulz, and D. Sala, "Application of mineral liberation analysis (MLA) for investigations of grain size distribution in submarine density flow deposits," *Marine and Petroleum Geology*, vol. 129, article 105109, 2021.

[22] S. Feng, Z. Xu, J. Chai, and Y. Li, "Using pore size distribution and porosity to estimate particle size distribution by nuclear magnetic resonance," *Soils and Foundations*, vol. 60, no. 4, pp. 1011–1019, 2020.

[23] X. Chen, G. Yao, E. Herrero-Bervera et al., "A new model of pore structure typing based on fractal geometry," *Marine and Petroleum Geology*, vol. 98, pp. 291–305, 2018.

[24] X. Chen, X. Zhao, P. Tahmasebi, C. Luo, and J. Cai, "NMR-data-driven prediction of matrix permeability in sandstone aquifers," *Journal of Hydrology*, vol. 618, article 129147, 2023.

[25] J. Chen, M. Gladkikh, S. Chen, D. Jacobi, and H. Kwak, "Determination of grain size distribution from NMR relaxation time using pore scale modeling," *International Symposium of the Society of Core Analysts*, vol. 3, no. 1, pp. 1–6, 2007.